NON-FOSTER IMPEDANCE MATCHING FOR ELECTRICALLY SMALL CAPACITIVE ANTENNAS

A THESIS

SUBMITTED TO THE DEPARTMENT OF ELECTRICAL AND

ELECTRONICS ENGINEERING

AND THE GRADUATE SCHOOL OF ENGINEERING AND SCIENCE

OF BILKENT UNIVERSITY

IN PARTIAL FULFILLMENT OF THE REQUIREMENTS

FOR THE DEGREE OF

MASTER OF SCIENCE

By

Şeyma Canik

August, 2014

I certify that I have read this thesis and that in my opinion it is fully adequate, in scope and in quality, as a thesis for the degree of Master of Science.

_____

Prof. Dr. Ayhan Altıntaş(Advisor)

I certify that I have read this thesis and that in my opinion it is fully adequate, in scope and in quality, as a thesis for the degree of Master of Science.

_____

Assoc. Prof. Dr. Vakur B.Ertürk

I certify that I have read this thesis and that in my opinion it is fully adequate, in scope and in quality, as a thesis for the degree of Master of Science.

_____

Prof. Dr. Mehmet Bayındır

I certify that I have read this thesis and that in my opinion it is fully adequate, in scope and in quality, as a thesis for the degree of Master of Science.

_____

Assist. Prof. Dr. Ali Kemal Okyay

I certify that I have read this thesis and that in my opinion it is fully adequate, in scope and in quality, as a thesis for the degree of Master of Science.

_____

Assist. Prof. Dr. Necmi Bıyıklı

Approved for the Graduate School of Engineering and Science:

_____

Prof. Dr. Levent Onural
Director of the Graduate School

iii

ABSTRACT

NON-FOSTER IMPEDANCE MATCHING FOR ELECTRICALLY SMALL CAPACITIVE ANTENNAS

Şeyma Canik

M.S. in Electrical and Electronics Engineering

Supervisor: Prof. Dr. Ayhan Altıntaş

August, 2014

Device scaling and component-miniaturization are the main drivers of the development of electronic technology. In time, electronic devices have become smaller in size and hence, the scaling down of antenna dimensions has come to be not only an interesting but also substantial areas of research. The gain - bandwidth product of an antenna is limited by its electrical size, therefore reducing the size of an antenna narrows the bandwidth or lowers the gain. The work presented in this thesis contributes to the existing body of research on the structure of electrically small antennas and complications of its design with regard to the fundamental limitations.

The large input reactance of electrically small antennas (ESA) are conventionally matched with passive circuits, however, the matching works at a single frequency which shrinks the bandwidth. In previous studies, non-Foster impedance matching which employs active networks of negative inductors and capacitors to overcome the restrictions of gain-bandwidth theory has been examined. In this study, the origins and development of Non-Foster impedance matching is reviewed and its stability issues are discussed. The design and simulation of a negative impedance converter circuit and together with an electrically small disk loaded dipole are presented. In this research, the designed matching circuit is fabricated, measured and its results are analyzed. Additionally, promising future studies and their possible effects in the antenna field are reviewed.

Keywords: Matching, ESA, Non-Foster, NIC, Disk Loaded Dipole.

ÖZET

ELEKTRİKSEL OLARAK KÜÇÜK KAPASİTİF ANTENLERİN NON-FOSTER EMPEDANS UYUMLANDIRMASI

Şeyma Canik
Elektrik ve Elektronik Mühendisliği Bölümü, Yüksek Lisans
Tez Yöneticisi: Prof. Dr. Ayhan Altıntaş
Ağustos, 2014

Cihaz ölçeklemek ve bileşen minyatürize etmek elektronik teknolojisinin gelişimi için temel yönelimlerdir. Elektronik cihazların boyutları zamanla küçülmektedir, buna bağlı olarak anten boyutlarını küçültmek ilgi çekici ve önemli bir araştırma alanına dönüşmektedir. Bir antenin kazanç-bant genişliği çarpımı elektriksel boyutuyla sınırlıdır, bu yüzden antenin boyutunu küçültmek bant genişliğini daraltır veya kazancı düşürür.

Elektriksel olarak küçük antenlerin (ESA) büyük girdi reaktansı geleneksel olarak pasif devre ile uyumlandırılır ancak uyumlandırma tek bir frekansta çalışır bu da bant genişliğini kısıtlar. Daha önceki çalışmalarda, kazanç-bant genişliği teorisinin kısıtlamalarını aşmak için negatif endüktans ve kapasitörler kullanan aktif non-Foster empedans uyumlandırma devreleri incelenmiştir. Bu çalışmada, non-Foster empedans uyumlandırmanın kökeni ve gelişimi incelenmiş ve kararlılık konuları ele alınmıştır. Bir negatif empedans dönüştürücü devresi tasarımı ve simülasyonu sunulmuştur. Devrede elektriksel küçük disk bağlı dipol anten kullanılmıştır. Tasarlanan uyumlandırma devresi üretilmiş, ölçülmüş ve sonuçları analiz edilmiştir. Ayrıca, gelecekte umut vadeden çalışmalar ve onların anten alanındaki olası etkileri tartışılmıştır.

Anahtar sözcükler: Uyumlandırma, ESA, Non-Foster,Disk Bağlı Dipol.

Acknowledgement

I am privileged to have the opportunity to undertake such a challenging, but yet rewarding Master of Science. It is indeed a highly gratifying experience to pursue this research through the beginning to the end.

I would like to take this opportunity to express my gratitude to my advisor Prof. Dr. Ayhan Altıntaş for his guidance and continuous encouragement during my research. I would like to thank Assoc. Prof. Dr. Vakur B. Ertürk for reviewing my research and providing fruitful insights during our discussion. I would also thank Prof. Dr. Mehmet Bayındır and Assist. Prof. Dr. Necmi Bıyıklı for their interest and for time for being a part of my defense committee. I especially thank to Assist. Prof. Dr. Ali Kemal Okyay for encouraging me to continue my academic studies when I was about to give up. Studying with him and his group for the last six months has been a tremendous experience for me. I sincerely thank Dr. Kağan Topallı for the time that he has dedicated to discussing my researches with me and being the most cordial and helpful instructor I know.

I thank my family for their unconditional love, support and prayers. Throughout my life, my father has been the personal mentor for me. He always believes in me and never gives up. I am grateful to my dear mother for her never ending self sacrifice and warmth. I thank my older brother, Ahmet for being a role model for me in diligence and for his support while in choosing this job and encouraging my academic career. I would also thank to his wife, Esra who is like a sister to me and she has always been there for me. Additionally, I send my love to their little princess who will join our family soon. I am greatly appreciative of my other charismatic brother, Enes Ulvi for his logistic supports (driving me to university everyday :)) and our enjoyable conversations. Also, I would like to thank to my uncles; Adv. Ümit Ulvi Canik who guided me with his reliable, decent, diligent personality and Abdulhakim Duman from whom I have inherited my curiosity in and fascination with science. I could not have achieved any of this without my family.

I would like to thank Elif Özgöztaşi Çelebi who has always stood by my side

dedicated to my father and my mother, their wisdom, courage and passion for education are inspiration to me

Contents

List of Figures

Chapter 1

Introduction

Modern communication devices have high market penetration and have become a common commodity. The demand for cellular systems, RFIDs, GPS systems and other wireless equipment has grown rapidly. Correspondingly, there has been a tremendous need for antennas occupying a small volume to reduce cost, increase mobility and functionality of wireless communication systems. Furthermore, because a single antenna is favored when handling multiple bands and radios such as multi-input multi-output (MIMO) mobile communications systems, the widest operating bandwidth of the antenna also has become an important component. Emerging broadband applications due to market pressures for miniaturized communication devices, have encouraged the use of electrically small antennas (ESA).

There is a distinction between the physical size and the electrical size of the antenna. An antenna can physically occupy a small volume, however, electrical smallness is related to the free space wavelength at the operating frequency. Generally speaking, an antenna is considered to be electrically small if it has a maximum physical dimension that is comparable to its wavelength. There have been various endeavors to specify the electrically smallness of an antenna. In the mid 20th century, Chu [2] and Wheeler [3] worked on the ESA and came up with a formula in which the ESA is an antenna that satisfies the condition;

$$ka < 0.5 \tag{1.1}$$

where k is the wave number defined as $2\pi/\lambda$, λ is the wavelength of the operating frequency and a is the radius of the minimum size sphere that encloses the antenna. The sphere is termed as the "Wheeler Cap".

Later, Hansen redefined the limit as [1];

$$ka < 1 \tag{1.2}$$

which is interpreted as an antenna enclosed inside a sphere with a radius equal to one radian length and the sphere is called a "radian sphere" [2].

The miniaturization of antennas concerns many wireless communication devices; however, minimizing the antenna size is subject to limitations, which directly affect the performance. The ESA is demanded to have a wide operational bandwidth, but without compromising the radiation efficiency or gain. As a matter of fact, there are tradeoffs between size, bandwidth, and efficiency. The fundamental limitation theory of the ESA was suggested by [1] [3] and [4] which state that the gain-bandwidth product of ESA is bounded. Hence, it is necessary to understand the theoretical limits in order to obtain an optimum design for maximum performance. Moreover, if there is a gap between the theoretical and practical limits, it is also crucial to understand how to modify the antenna design to reduce the gap.

In order to understand the limitation imposed on an ESA, one should understand the antenna parameters and their relations with size. The length and size of antennas are generally chosen as multiples of half wavelength ($\lambda/2$)[5]. The resonant length implies real terminal impedance, at this length it is easy to match the antenna to a transmission line which is connected to it. However, ESA is characterized by a large reactance and small resistive part of the input impedance which implies a high quality factor (Q-factor). The large reactance part behaves capacitively and stores most of the energy and restrains power to radiate. Thus, the ESA requires an external matching network. The classic

matching includes passive elements which posses positive impedance. Inductors are conventionally used for matching, however, total reactance vanishes only at a single frequency which shrinks the range of operation and hence the antenna becomes a very narrow band.

Recently, non-Foster impedance matching has been proposed which employs active components to match the reactive part of the antenna impedance over a broad frequency range. In 1924, Ronald M. Foster introduced a theorem which suggested that the frequency derivative of the reactive part of the circuit is always greater than zero, i.e. reactive part of system monotonically increases with frequency for a 2-terminal passive and lossless network [6]. A negative impedance converter (NIC) circuit uses non-Foster elements which have a negative reactance slope. The circuit behaves like negative inductors or negative capacitors which are able to cancel out the reactance part of an antenna impedance over a wider range of frequencies. Using non-Foster impedance matching, the limitation of a gain-bandwidth product can be overcome. A lot of work had been suggested over the years and, although the technology of NIC is old, the practical and novel studies in Non -Foster matching have been recently published. S.E. Sussman is one of the great contributors who suggested the matching for electrically small dipole, monopole and blade antennas[7], [8]. Non-Foster matching of leaky-wave antennas and series-fed antenna arrays are suggested in [9] and active metamaterial based on non-foster elements are studied in [10]. Also, many research papers have been written on stability concern, such as [11], [12] and [13].

The motivation of this thesis is overcoming the gain-bandwidth limitation of ESA using Non-Foster elements, hence, designing portable and efficient disk loaded dipole antenna in RF. The Non-Foster matching is a promising area of research which provides smaller dimensions with broadband and high gain ESA.

The organization of this thesis is as follows. After introductory information, literature review and motivation, Chapter 2 starts with the introducing fundamental parameters of antennas such as radiation, radiation pattern, stored energies, quality factor, gain and bandwidth. The relation between these parameters is explained and the fundamental gain-bandwidth limitation of ESA is introduced

and the necessity of a matching network is discussed. Then, the equivalent circuit model of ESA is analyzed and suggested. In the last part of the chapter, disk loaded dipole is investigated in the frequency range of 20-110 MHz and the simulation results along with their interpretations are given.

In Chapter 3, two types of external matching are provided; a passive and an active matching. Then, their performance are compared in terms of the Q-factor. The literature survey for a transistor based NIC circuit is described. Then, the equivalent circuit model of BJTs is shown and explained. A brief history of the NIC is stated and the examples of previous works are detailed. In order to match designed disk loaded dipole antenna, a NIC circuit with non-Foster elements are constructed and simulated. At the end of Chapter 3 the stability issues are discussed.

Chapter 4 is dedicated to simulation fabrication and measurement results of the antenna and the matching circuit. The designed NIC circuit is fabricated on a board. The ESA is represented by the equivalent circuit model as a single capacitor and a resistor, then, connected to the negative capacitor circuit. The measurements are taken with a vector network analyzer based on scattering (S) parameters. The thesis is briefly summarized in the last chapter.

Chapter 2

Electrically Small Antennas

2.1 Fundamental Parameters

In order to find an optimal design of ESA for a particular application, basic antenna parameters should be analyzed and their relationship should be investigated. This chapter introduces definitions of necessary parameters for designing ESAs, as well as basic circuit model for them. After comparisons of the certain characteristics of the monopole, dipole and the disk loaded dipole ESAs, the chapter is concluded with the design and simulation of the disk loaded dipole antenna.

2.1.1 Radiation and Radiation Pattern

According to *IEEE Standart Definitions of Terms for Antennas* electromagnetic (EM) radiation was defined as an emission of electromagnetic energy from a bounded region in the form of unguided waves [14]. It is basically originated from accelerating electrons. An antenna can be defined any object that converts electrical energy to radiation. The antenna working principle can be basically explained as follows: a current applied upon a conductor excites the electrons around the nucleus and then loses its extra energy by emitting electromagnetic

radiation and hence falls back into its original energy level. The frequency of the radiated waves depends on the energy levels of electrons around the nucleus. According to Planck's law the wavelengths of rays are inversely proportional to energy which means the smaller the wavelength is the larger the energy it carries. The radiated EM waves have speeds depending on the medium they are passing through and in a vacuum they are traveling at the speed of light which is a universal constant of $c = 3x10^8 m/sec$.

The radiation pattern is the variation in the strength of radiated power from an antenna as a function of spherical coordinates. An antenna can be characterized in three regions; reactive near field, radiating near field and far field as a function of radial distance. As we go further away from the antenna in space or in the area, after a certain point the angular field distribution is no longer dependent on radial distance and this region is accepted as the far field. Therefore, in the far field the radiation pattern only depends on azimuth and elevation angles.

The radiation power pattern is normalized to its maximum value and is generally expressed in a logarithmic scale which has a unit of decibel (dB). The decibel is a dimensionless unit so power expressed in dB must be normalized.

$$Power\ in\ dB = 10 \log_{10} Power/PeakPower \qquad (2.1)$$

For an infinitesimal linear z-directed wire antenna, which is excited by a uniform current I_0, radiated fields are found by solving a vector potential equation and making the appropriate approximation.

$$\mathbf{A}(x,y,z) = \frac{\mu}{4\pi} \int_c \mathbf{I}_e(x',y',z')\frac{e^{-jkR}}{R}dl' = \hat{a}_z \frac{\mu I_0}{4\pi r}e^{-jkr} \int_{-l/2}^{l/2} dz' = \hat{a}_z \frac{\mu I_0 l}{4\pi r}e^{-jkr}$$

$$(2.2)$$

Using symmetry of the wire antenna(no ϕ variation) and the transformation from the cartesian to spherical coordinates, the components of vector potential are found as;

$$A_r = A_z \cos\theta = \frac{\mu I_0 l e^{-jkr}}{4\pi r} \cos\theta \tag{2.3}$$

$$A_\theta = -A_z \sin\theta = -\frac{\mu I_0 l e^{-jkr}}{4\pi r} \sin\theta \tag{2.4}$$

$$A_\phi = 0 \tag{2.5}$$

Magnetic field intensity ($\mathbf{H}$) due to the vector potential ($\mathbf{A}$) is given as

$$\mathbf{H} = \frac{1}{\mu}\boldsymbol{\nabla} \times \mathbf{A} \tag{2.6}$$

Substituting 2.3, 2.4 and 2.5 into 2.6 it reduces into [5]

$$H_r = H_\theta = 0 \tag{2.7}$$

$$H_\phi = j\frac{k I_0 l \sin\theta}{4\pi r} e^{-jkr}[1 + \frac{1}{jkr}] \tag{2.8}$$

In the far fields only the first term prevails. Using the formula that relates the magnetic field and the electric field

$$\mathbf{E} = -j\omega\boldsymbol{A} - j\frac{1}{\omega\mu\epsilon}\boldsymbol{\nabla}(\boldsymbol{\nabla}\cdot\mathbf{A}) = \frac{1}{j\omega\mu\epsilon}\boldsymbol{\nabla}\times\mathbf{H} \tag{2.9}$$

One can obtain the corresponding electric field components;

$$E_r = \eta\frac{I_0 l \cos\theta}{2\pi r^2}e^{-jkr}[1 + \frac{1}{jkr}] \tag{2.10}$$

$$E_\theta = j\eta\frac{k I_0 l \sin\theta}{4\pi r}e^{-jkr}[1 + \frac{1}{jkr} - \frac{1}{(kr)^2}] \tag{2.11}$$

$$E_\phi = 0 \tag{2.12}$$

The total radiated power is calculated by integrating the real part of the Poynting vector over a spherical surface of any radius

$$P_{rad} = \frac{1}{2}\int_s Re(\mathbf{E}\times\mathbf{H}^*)\cdot\mathbf{ds} \tag{2.13}$$

$$= \frac{1}{2}\left(\frac{k I_0 l}{4\pi}\right)^2\int_0^{2\pi}\int_0^\pi \eta\frac{\sin^2\theta}{r^2}r^2\sin\theta drd\theta d\phi = \eta\frac{(k I_0 l)^2}{12\pi} \tag{2.14}$$

As it can be seen, radiated power is proportional to the square of the length. Thus, miniaturization is unfavorable for radiated power.

7

2.1.2 Stored Energies

While some of the input power is radiated, some of it is stored in the region around the antenna. In order to calculate the stored energies, one must find the energy densities first. Electrical energy densities are obtained from the electric field in the form of

$$\omega_e = \frac{1}{2}\epsilon \mathbf{E} \cdot \mathbf{E}^* = \frac{1}{2}\epsilon(|E_r|^2 + |E_\theta|^2) \tag{2.15}$$

Calculating and writing in more compact form, we get

$$\omega_e = \eta \frac{1}{2\omega}\left(\frac{kI_0l}{4\pi}\right)^2 [\sin^2\theta\left(\frac{k}{r^2} - \frac{1}{kr^4} + \frac{1}{k^3r^6}\right) + 4\cos^2\theta\left(\frac{1}{k^3r^6} + \frac{1}{kr^4}\right)] \tag{2.16}$$

Magnetic energy density is found in the same way

$$\omega_m = \frac{1}{2}\mu \mathbf{H} \cdot \mathbf{H}^* = \frac{1}{2}\mu|H_\phi|^2 \tag{2.17}$$

Putting 2.8 to the equation, we can find the total magnetic energy density as;

$$\omega_m = \frac{1}{2}\mu\left(\frac{kI_0l\sin\theta}{4\pi}\right)^2\left(\frac{1}{r^2} + \frac{1}{k^2r^4}\right) \tag{2.18}$$

The electric energy density associated with the traveling wave is the propagating energy density; that is, the energy calculated from the field components which produce the radiated power. The propagating energy density, ω_e^{rad} is computed using only the far field expressions [15]

$$H_\phi^{rad} = \sin\theta\frac{jkI_0l}{4\pi r}e^{-jkr} \tag{2.19}$$

The radiated electric field $\mathbf{E}$ can be found using 2.9

$$E_\theta^{rad} = j\eta\sin\theta\frac{kI_0l}{4\pi r}e^{-jkr} \tag{2.20}$$

The density of electrically stored energy computed from the radiated field

$$\omega_e^{rad} = \frac{1}{2}\epsilon |E_\theta^{rad}|^2 = \eta^2 \epsilon \left(\frac{kI_0 l}{4\pi}\right)^2 \frac{\sin^2\theta}{2r^2} \tag{2.21}$$

Subtracting the propagating energy density from the total radiated electrical energy density we obtain the non-propagating energy density

$$\omega_e^{stored} = \omega_e - \omega_e^{rad} \tag{2.22}$$

$$= \eta \frac{1}{2\omega}\left(\frac{kI_0 l}{4\pi}\right)^2 [\sin^2\theta\left(\frac{1}{kr^4} - \frac{1}{k^3 r^6}\right) + 4\cos^2\theta\left(\frac{1}{kr^4} + \frac{1}{k^3 r^6}\right)] \tag{2.23}$$

Total non-propagating (stored) energy density is found by taking the integral over an infinite sphere

$$W_e^{stored} = \int\limits_0^{2\pi}\int\limits_0^{\pi}\int\limits_a^{\infty} \omega_e^{stored} r^2 \sin\theta dr d\theta d\phi \tag{2.24}$$

$$= \frac{\eta}{3\omega}\frac{(kI_0 l)^2}{4\pi}\left(\frac{1}{ka} + \frac{1}{k^3 a^3}\right) \tag{2.25}$$

where a is the radius of the minimum sphere which encloses the antenna.

One can apply the same steps for magnetic radiated energy density to get

$$\omega_m^{rad} = \frac{1}{2}\mu |H_\phi^{rad}|^2 = \frac{1}{2}\mu \left(\frac{kI_0 l \sin\theta}{4\pi}\right)^2 \frac{1}{r^2} \tag{2.26}$$

and

$$\omega_m^{stored} = \omega_m - \omega_m^{rad} = \frac{1}{2}\mu \left(\frac{I_0 l \sin\theta}{4\pi}\right)^2 \frac{1}{r^4} \tag{2.27}$$

The total stored magnetic energy is found by taking the integral

$$W_m^{stored} = \int\limits_0^{2\pi}\int\limits_0^{\pi}\int\limits_a^{\infty} \frac{1}{2}\mu \left(\frac{I_0 l \sin\theta}{4\pi}\right)^2 \frac{1}{r^4} r^2 \sin\theta dr d\theta d\phi \tag{2.28}$$

$$= \eta \frac{\omega(I_0 l)^2}{12\pi}\frac{1}{ka} \tag{2.29}$$

9

2.1.3   Quality (Q) Factor

The quality (Q) factor is a figure of merit that is used to relate stored and lost energy. It is defined as the ratio of the energy stored in the fields excited by the antenna to the energy radiated and dissipated per cycle multiplied by 2π [14]

$$Q = 2\pi \frac{\text{Energy Stored}}{\text{Energy dissipated per cycle}} = 2\pi f \frac{\text{Energy Stored}}{\text{Power Loss}} \tag{2.30}$$

Wheeler introduced the electrical length of the antenna as the axial length of a cylinder that circumscribes the antenna [4]. In later work, Chu [3] and Harrington [16] used spherical mode theory and defined electrical length as the radius of a circumscribing sphere that encloses the antenna with minimum radius that was represented with a. Wheeler and Chu defined the radiated minimum achievable Q-factor for linearly polarized wire antenna as follows [3],[4];

$$Q = \begin{cases} \omega_0 W_e^{stored}/P^{rad} & \text{if } W_e^{stored} > W_m^{stored} \\ \omega_0 W_m^{stored}/P^{rad} & \text{if } W_m^{stored} > W_e^{stored} \end{cases} \tag{2.31}$$

ESA has stored electrical energy higher than the stored magnetic energy, therefore the first condition is applied. Putting the results of equation 2.25 and 2.14 into the equation 2.32, the Q-factor of electrically small dipole antenna is found as;

$$Q = \omega_0 \frac{W_e^{stored}}{P^{rad}} = \frac{1}{ka} + \frac{1}{k^3 a^3} \tag{2.32}$$

Equation 2.32 relates the maximum linear dimension of an antenna to the minimum achievable Q-factor. Since a is very small, and Q is proportional to the third power of the length, an ESA has a high Q-factor.

All of the studies have concurred that the ESAs, independent of their shape

and type, have a high Q-factor, and consequently are difficult to match. Minimizing the Q-factor is essential for improving the performance of the ESA. The optimization of the antenna dimensions or/and external matching circuit is required in order to decrease the Q-factor and increase the radiated power. Furthermore, gain and bandwidth are also related to the Q-factor and a high Q-factor puts restriction on them.

2.1.4   Bandwidth

Bandwidth is one of the important parameters for antenna characterization. One can define the fractional bandwidth in terms of the Q-factor of an antenna as

$$FBW = \frac{\Delta f}{f_0} = \frac{1}{Q} \tag{2.33}$$

where f_0 is the center frequency and Δf is the operating 3dB bandwidth of an antenna. 2.33 is a suitable approximation where $Q \gg 1$ [7].

Equation 2.33 together with 2.32 implies the fundamental restriction on the bandwidth of ESA. While the antenna dimensions are getting smaller, the Q-factor is increasing and hence the operating bandwidth becomes narrower.

2.1.5   Gain

ESA has a high Q-factor characterized by a large reactance and small radiation resistance. The large capacitive reactance acts to store much of the input power, therefore only a small amount of power is radiated [4]. Consequently, miniaturization which is unfavorable for radiation efficiency imposes restriction on the gain. When the antenna gets smaller in size some of its properties and its performance becomes limited.

In his work, Harrington [16] defined the practical upper limit for the maximum gain that an antenna can achieve as;

$$G = (ka)^2 + 2ka \qquad (2.34)$$

where $ka > 1$ and the antenna satisfies the assumption of having at least one propagating mode. Harrington claimed that antennas with a gain greater than this limit, are classified as super-gain antenna. For a super gain antenna, the bandwidth is poor and due to the high field intensities of the antenna structure, losses are excessive [17]. For ESA ($ka < 1$), gain is often difficult to quantify correctly and we do not have a reasonable formula for that. However, it is widely accepted to consider the maximum linear gain of 3, regardless of its size [16]. We can conclude that the gain of ESA has an upper limit. After all, decreasing the dimension of the antenna puts restriction on the gain. We need to maximize the gain and at the same time widen the bandwidth to obtain efficient, high performance ESA.

2.1.6 Scattering Parameters

In order to analyze the performance of the ESA and the matching circuit, we need to understand some other parameters. In two port networks, scattering (S) parameters are used as mathematical expressions introduced by Vitold Belevitch in 1945 [18] that contain information about the electromagnetic behavior of the network. Using the matrix notation of S parameters provides us simplicity.
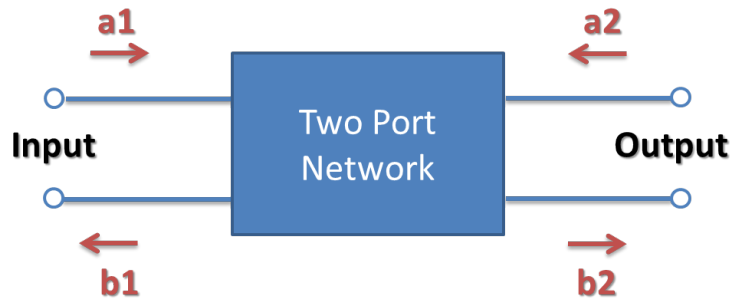

Figure 2.1: Two Port Network

According to Figure 2.1, a_n and b_n represent incident and reflected wave amplitudes respectively. S parameters are defined in terms of a_n and b_n as

$$\begin{pmatrix} b_1 \\ b_2 \end{pmatrix} = \begin{pmatrix} S_{11} & S_{12} \\ S_{21} & S_{22} \end{pmatrix} \begin{pmatrix} a_1 \\ a_2 \end{pmatrix} \tag{2.35}$$

S parameters contain information about network parameters. S_{11} is related to input return loss (RL) as;

$$RL_{in} = -20 \log_{10} |S_{11}| dB \tag{2.36}$$

Return loss is a measure of effectiveness of the delivered input power transmitted to the load, i.e. its the ratio of the incident power to the reflected power. It represents the reduction in the amplitude of the reflected wave in comparison to the incident wave [19]. It is generally expressed in dB. High RL implies a better match and higher load power. It is always a positive and non-dissipative value in passive networks, however, it can be negative in active circuits which impose energy into the circuit.

Conversely, the amplitude ratio of a reflected wave relative to that of the incident wave is called the reflection coefficient (Γ). It is the negative sign of the return loss in dB scale.

Voltage Standing wave ratio (VSWR) is defined as the ratio of maximum to minimum voltage amplitude in a standing wave pattern. It is a measure of an impedance mismatch between the transmission line and its load. The higher the VSWR, the greater the mismatch. The minimum VSWR which corresponds to a perfect impedance match, is unity, i.e. voltage amplitudes do not change in a standing wave pattern [20]. The VSWR is defined as;

$$VSWR = \frac{1 + |S_{11}|}{1 - |S_{11}|} \tag{2.37}$$

S_{12} and S_{21} represents forward and reverse gain respectively which are measured in dB. Insertion loss (IL) is the ratio of the power delivered to the line following the device to the power delivered to that part before insertion.

$$IL = -20 \log_{10} |S_{21}| dB \qquad (2.38)$$

In reciprocal passive network; $S_{main} = S_{NM}$ i.e. the S matrix is equal to its transpose.

The last parameter S_{22} similar to S_{11} but this time we are concerned with the wave amplitudes at the output port.

$$RL_{out} = -20 \log_{10} |S_{22}| dB \qquad (2.39)$$

2.2 Basic Circuit Model

The main goals in antenna design are achieving a good impedance matching, thereby getting low VSWR, high radiation efficiency and wide operating bandwidth. An ideal antenna should satisfy 1:1 VSWR over a desired frequency range and an efficiency approaching to 100%. However, due to the gain-bandwidth limitation of the ESA, it is hard to obtain these values. We need to obtain reasonably well matching over a wide frequency range.

ESA matching can be performed in two different ways; external matching network and modification of the antenna structure. External matching networks are going to be explained in later chapters. Changing the antenna geometry is more preferable than external matching since it has better performance. Wire antenna structures can be formed by the use of capacitance or top hat loading [21], inductive loading [22], multiple folded arms [22], [23] and metamaterials.

Feed point impedances of ESA are in the form of $Z_A = R_A - jX_A$ where $X_A \gg R_A$. The negative reactive part implies that the equivalent capacitance

14

dominates and reactance is proportional to $1/\omega C$. The large capacitive reactance acts to store much of the energy therefore a small amount of power is radiated. In order to overcome this problem, matching is required. To mitigate the capacitive part and to make the antenna self resonant, the structure of an antenna can be modified to include either a combination of capacitive top hat or inductive loading by increasing the wire length [24].

In this study the impedance properties of some known types of antennas were compared. These include the monopole, dipole and disk loaded dipole ESAs. These antennas have the advantage of easy fabrication and simulation. In addition, they are omnidirectional in the horizontal plane, which means they radiate the same amount of power in all directions in the plane.

First of all lets start with the characteristics of a dipole antenna. In this part, we refer to section 10.3 of [25].

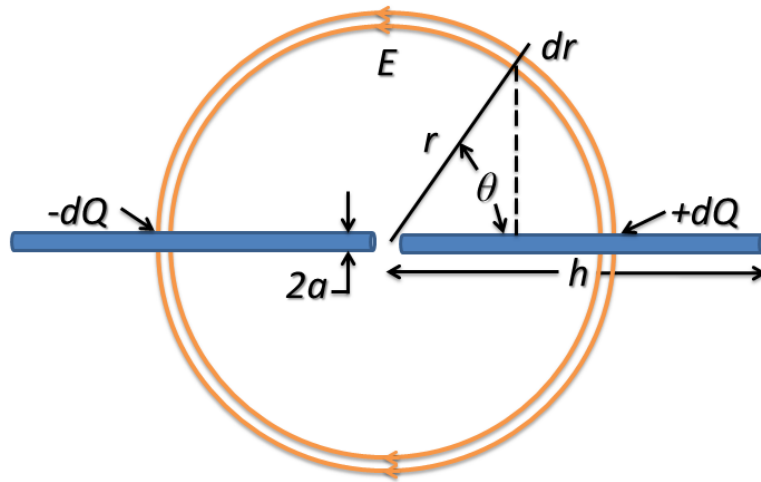Figure 2.2: Short, Center-Fed, Linear Dipole Antenna

Assuming that the electric field lines follow the semicircular path from one arm to the other arm of the dipole antenna and that the field lines emanating from charge dQ in interval dr at distance r from the feed point of the antenna cross a surface area of $2\pi r \, dr \, \sin\theta$ that lies on a cone of half angle θ as seen from

15

the Figure 2.2. The electric field strength at (r, θ) is then calculated as

$$E = \frac{dQ/dr}{2\pi\epsilon_0 r \sin\theta} \tag{2.40}$$

The voltage difference across the two arms of the dipole is[26]

$$\Delta V = 2 \int\limits_{\theta_{min}}^{\pi/2} Erd\theta = \frac{dQ/dr}{\pi\epsilon_0} \ln(2r/a) \tag{2.41}$$

Making appropriate approximations we obtain the capacitance as [25]

$$C \approx \frac{\pi\epsilon_0 l}{\ln(l/a)} \tag{2.42}$$

The magnetic field around the line carrying a current which drops from I to 0 over the length l of each arm is

$$B = \frac{\mu_0 I_0}{2\pi r} \tag{2.43}$$

The total magnetic flux of the wire antenna

$$\Phi = l \int\limits_{a}^{l} Bdr = \frac{\mu_0 l I_0}{2\pi} \ln\frac{l}{a} = L I_0 \tag{2.44}$$

Then the estimated inductance value of the antenna is found as;

$$L \approx \frac{\mu_0 l}{2\pi} \ln\frac{l}{a} \tag{2.45}$$

The total reactance of the short linear dipole

$$X_A = \omega L - \frac{1}{\omega C} \approx \frac{\mu_0 \omega l}{2\pi} \ln\frac{l}{a} - \frac{1}{\pi\epsilon_0 \omega l} \ln\frac{l}{a} = \frac{\mu_0 c l}{\lambda} \ln\frac{l}{a} - \frac{\lambda}{2\pi^2 \epsilon_0 c l} \ln\frac{l}{a} \tag{2.46}$$

The first term, coming from inductive impedance, can be disregarded when the length of the antenna is smaller compared to the wavelength. This implies that the reactance of the antenna is mainly capacitive.

$$X_A \approx -\eta_0 \frac{\lambda}{2\pi^2 l} \ln(l/a) \tag{2.47}$$

The radiation resistance of the antenna can be found from radiated power

16

$$P_{rad} = \eta \frac{4\pi}{3} \left(\frac{kI_0 l}{4\pi} \right)^2 = \frac{1}{2} I_0^2 R_{rad} \qquad (2.48)$$

$$R \approx \eta \frac{8\pi}{3} (kl)^2 \qquad (2.49)$$

The input resistance of the antenna is a summation of radiation resistance and loss resistance.

$$R_{in} = R_{rad} + R_{loss} \qquad (2.50)$$

The radiation loss is given as;

$$R_{loss} = \frac{L}{6\pi a} \sqrt{\frac{\pi f \mu}{2\sigma}} \qquad (2.51)$$

In ESA, the inductance of the antenna (L) is responsible for the loss resistance which is very small for an ESA. Hence it is negligible, which means that the input resistance can be approximated as radiation resistance alone.

As stated in Wheeler et al. [4] the equivalent-circuit reactance of an electrically-small antenna increases linearly with decreasing electrical length. Also, the Q-factor can be expressed in terms of the feed-point resistance and reactance of an antenna [27]

$$Q = \frac{\omega_0}{2R} \sqrt{\left(\frac{\partial R}{\partial \omega} \right)^2 + \left(\frac{\partial X}{\partial \omega} + \frac{|X|}{\omega} \right)^2} \qquad (2.52)$$

where it can be approximated as the $Q = |Im(Z_{in})/Re(Z_{in})| = |X/R|$ [7]. As it is expected an ESA with a very high reactance and a small resistance has a high Q-factor.

2.3   Designed Antenna

The impedance characteristics of some monopole, dipole and disk loaded dipole ESA are given in Figure 2.3. The dipole and the disk loaded dipoles have the
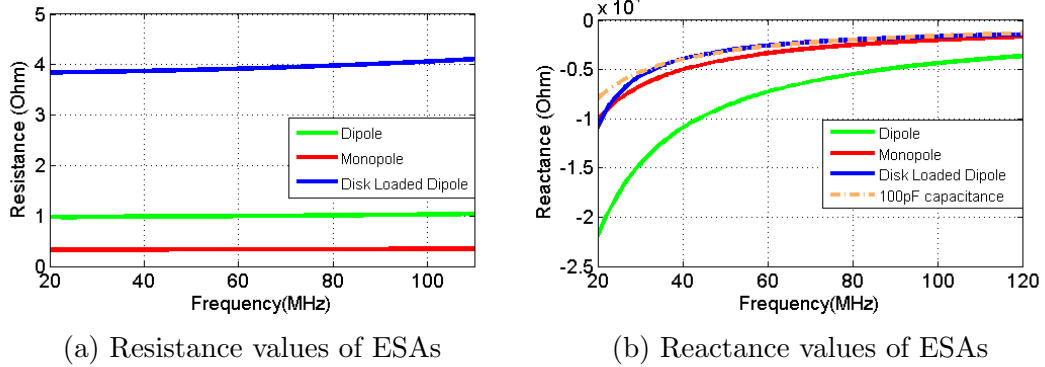
(a) Resistance values of ESAs   (b) Reactance values of ESAs

Figure 2.3: Comparison of ESA Input Impedances for Monopole, Dipole and
Disk Loaded Dipole Antennas[1]

same length and the length of the monopole antenna is half their length. As
it can be inferred from the reactance plot, the disk loaded dipole has a smaller
reactance value than the dipole, which means that the radiated energy of the
disk loaded dipole is higher than the dipole antenna. The monopole antenna has
a reactance value near to the value close to the disk loaded dipole, however, its
radiation resistance (ignoring the loss resistance) is smaller than the disk loaded
dipole. Consequently, in order to have a high radiation resistance with small
dimensions, the disk loaded dipole antenna is the favorable choice of an antenna.

The simulation of the antenna is performed using a 3D electromagnetic high-
frequency simulation tool of Ansoft HFSS. HFSS uses the finite element method
(FEM) to solve the electromagnetic structural problem. The FEM is a numeri-
cal technique for finding approximate solutions to boundary value problems for
differential equations. It uses variational methods to minimize an error function
and reach a stable solution. Finite element analysis (FEA) uses mesh generation
techniques to divide a complex problem into small elements. The HFSS uses the
software program coded with FEM algorithm, divides the space into tetrahedrons
and uses adaptive passes to converge for a given error limit[28].

The disk loaded antenna is 83.6 mm long, it has a radius of 0.707 mm and
the top loaded disks have a radius of 42 mm. The antenna is simulated in the

---

[1]The dipole and the disk loaded dipole ESA have the same lengths and the monopole antenna
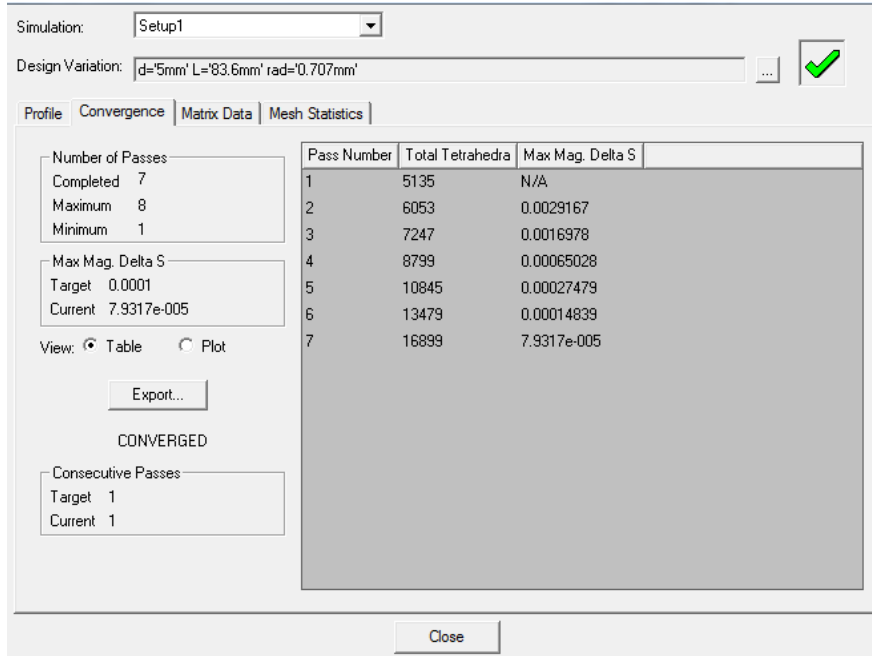is half of them

Figure 2.4: Convergence of the Simulation with HFSS simulation tool

range of 20-120 MHz with the center frequency of 70 MHz. Figure 2.4 shows the convergence of the simulation. The HFSS used 7 adaptive passes to reach the tolerable error limit.

Figure 2.6a shows the simulated disk loaded antenna and its radiation pattern. The advantage of this design is that a reduced length dipole was formed by capacitive or disk loading at the end of the conductors [29]. With the end-loading, the capacitance of the dipole increases between the upper and lower dipole arms, resulting in a decrease in the magnitude of the feed-point capacitive reactance. With an appropriate value of capacitance determined by the disk diameter the small dipole could be made self-resonant. Disk loaded dipole does not provide sufficient inductance to achieve self-resonance in our frequency range 20-120 MHz (VHF). As it can be seen from the figure, the radiated power value is very small because the power is stored and cannot be radiated. Hence, an external matching circuit is required to match the ESA that cancel out the reactive part of a terminal impedance to increase the gain of the antenna over a wide/broad frequency range.

As it seen from the Figure 2.6, the resistive part of the terminal impedance of

(a) Resistance

(b) Reactance
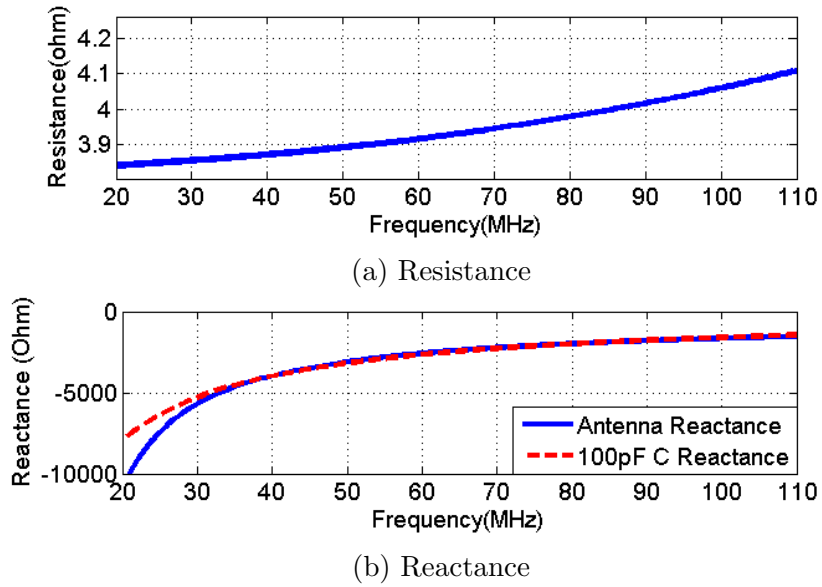
Figure 2.5: Input Impedance of Disk Loaded Dipole

the simulated disk loaded dipole has the value nearly 4 Ω over the interested frequency range. Also, the reactive part of the terminal impedance shows capacitive behavior which has well agreement with the reactance of the 100 pF capacitance for the values of frequencies higher than 30 MHz.
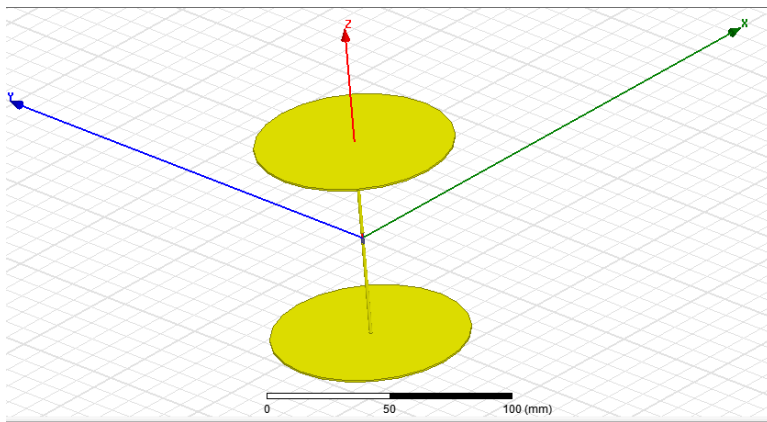
(a) Simulated Disk Loaded Dipole Antenna at 70 MHz, the length is 8.32 mm
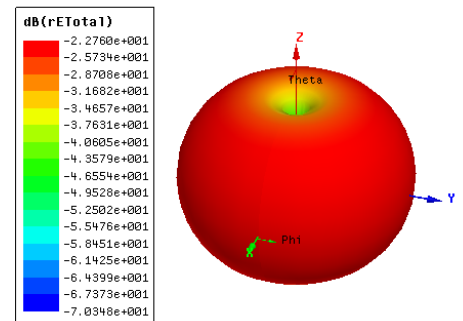
(b) Radiation Pattern of Disk Loaded Dipole Antenna

Figure 2.6: Simulated Disk Loaded Dipole ESA and Its Radiation Pattern

Chapter 3

Non-Foster Matching

3.1 Passive vs. Active Matching

As it is mentioned in the previous chapter, ESA has a high Q-factor character-
ized by a large reactance and a small radiation resistance. The large capacitive
impedance acts to store most of the energy, therefore only a small amount of
power is radiated. The main task is to match the impedance of ESA to a con-
stant resistance value which is typically 50 Ω . Conventional matching includes
lossless capacitors and inductors. However, such matching may not be sufficient
since passive components operate over comparatively smaller bandwidths than
ESA, which already has a high Q-factor. In some cases using no matching at all
performs better [30], [31]. Although, wideband matching can be obtained though
passive circuits, every component contributes to the total loss, hence the power
transferred to the antenna decreases and the efficiency lessens. In conclusion,
conventional matching either results in narrow bandwidth or low efficiency.

The conventional matching of ESA is done by passive circuits which cancels
out the negative reactance (capacitive impedance) of an antenna with an inductive
component and transform the overall impedance into a purely resistive value.
Although this approach can provide a very good match, it works at a single
frequency as in Figure 3.1(a). Therefore, the effectiveness of passive matching is
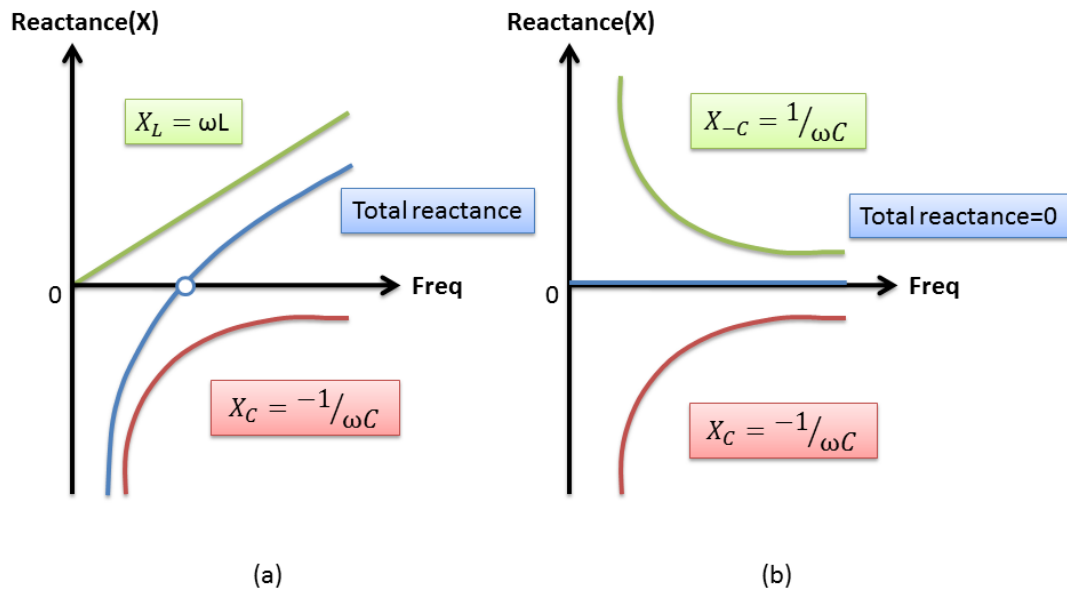
Figure 3.1: Passive vs. Active Matching of ESA

severely limited by the gain-bandwidth theory which constrains the antenna with either a narrow bandwidth and/or poor gain.

In order to overcome the deficiencies in passive matching, it is feasible to match the antennas with the circuit of Non-Foster elements. In 1924, Ronald M. Foster came up with a theorem which stated that the frequency derivative of the reactance of a system is always greater than zero, i.e. the reactive part of a system monotonically increases with the frequency of a two terminal passive and lossless network. One of the fundamental characteristic that makes a non-Foster element so novel is its negative reactance slope. On a Smith chart, this property corresponds to the impedance locus proceeding counter-clockwise towards the generator, with increasing frequency.

In the literature negative capacitors and inductors are the commonly used non-Foster components. Negative impedance converter circuits are constructed using these elements. Figure 3.1b shows how an ideal negative capacitor can cancel out a positive capacitance C over all frequencies, as compared to the usual method of resonating C at a single frequency with a positive inductor L as in 3.1b. This

approach can be extended in an idealized process called negative-image modeling, whereby an electrically-small antenna is matched to 50 Ω over all frequencies [8]. Initially, the total antenna impedance is turned into a frequency-squared-dependent radiation resistance as it is calculated in the previous chapter. This resistance value can be matched into a constant 50 Ω via conventional methods.

The negative impedance converter (NIC) uses active elements such as op-amps or transistors to obtain the negative of the load impedance at the input. Since the impedance is almost frequency independent, the matching operates at a very large frequency range which implies a wider bandwidth. This matching allows greater radiated power, as compared to a conventional case, without increasing the transmitter power. Applying proper bias, non-Foster matching achieves a significant advantage in the overall power efficiency.

3.2   Equivalent Circuit Model

As in the ESA design, the equivalent circuit concept has an advantage in RF frequencies while analyzing the total system. NIC circuits use Bipolar Junction Transistors (BJTs) for voltage conversion. The BJT consists of two PN-junctions producing three connecting terminals which are known and labeled as the emitter (E), the base (B) and the collector (C) respectively. BJTs are current regulating devices that control the amount of current flowing through them in proportion to the amount of biasing voltage applied to their base terminal, acting like a current-controlled switch [32]. It has two types; NPN and PNP which have exactly the same structure, but a different order of doped materials. This reflects their biasing and the polarity of the power supply. NPN transistors consist of a layer of P-doped semiconductor, which is the base, between two N-doped layers and PNP transistors consist of a layer of N-doped semiconductor between two P-doped layers. Transistors can act either as insulators or conductors by the application of a small signal voltage. Transistors are able to change between these two states which enable them to have two basic functions: switching (digital electronics) or amplification (analogue electronics). Then Bipolar Transistors have the features

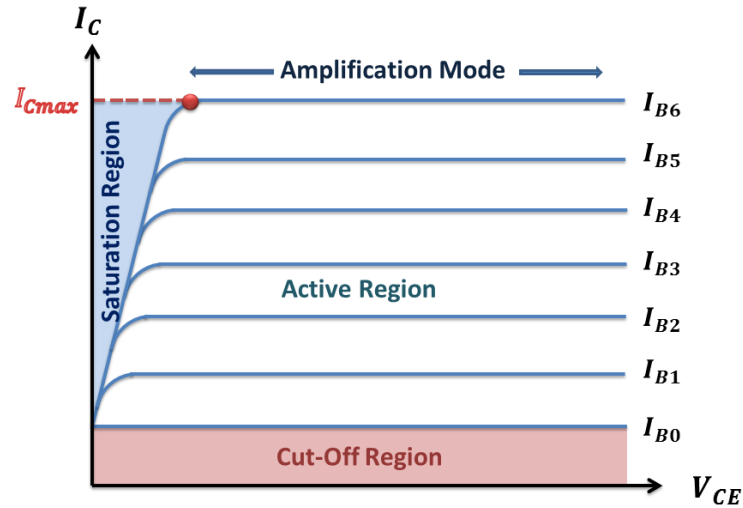to operate within three different regions and one non-operable region:

Figure 3.2: BJT Operating Range

- **Active Region**: the transistor operates as an amplifier. Most bipolar transistors are designed to afford the greatest common-emitter current gain (β) in forward-active mode. For NPN BJT transistors the B-E junction is forward biased and the C-E junction is reverse biased (opposite for PNP). $I_c = \beta I_b$ and $V_{CC} > V_{CE} > V_{BE}$. In reverse active mode or inverse mode, transistors have a similar function, however the emitter and collector have opposite behaviors

- **Saturation Region** : The Applied base voltage is higher than the voltage of the emitter and the collector. The B-E and B-C junction is forward biased for NPN (reverse for PNP). I_C reaches a maximum value which is independent of I_B and β. In this region we do not have a control mechanism for current regulation. The transistor is fully ON operating as a switch and $I_C = I_{cmax}$

- **Cut-off Region** : The base-emitter junction is the reverse biased. Current does not flow and the transistor is fully OFF. It is operating as a switch and $I_C = 0$

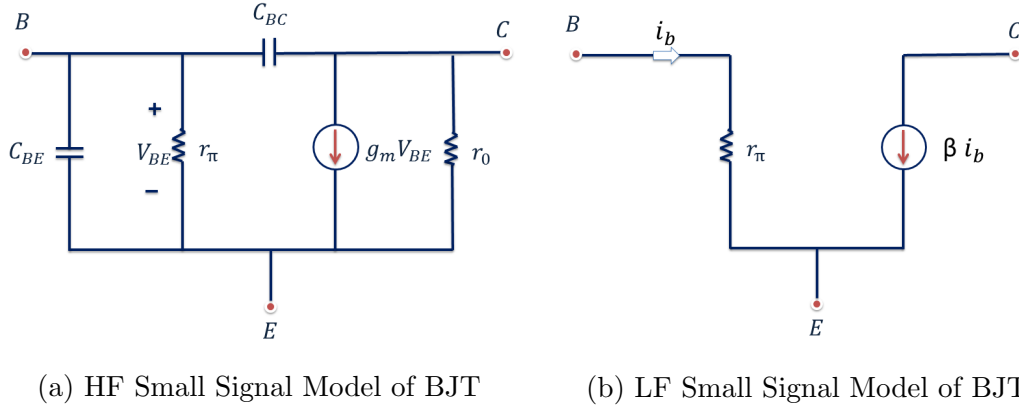(a) HF Small Signal Model of BJT   (b) LF Small Signal Model of BJT

Figure 3.3: Hybrid-pi Equivalent Circuit Model of BJT

- **Breakdown Region** : If I_c and V_{CE} exceed given specifications, the transistor cannot operate properly and can be damaged.

In this work, we used forward active region in order to use BJT as an amplifier and from the above Figure 3.2 we can control the amplification level with the base current I_b. In that figure the amplification level increases with the base current level ($I_{b6} > I_{b5} > I_{b4} > ... > I_{b0}$) This control is provided by proper biasing.

It is feasible to use circuit theory when analyzing the circuit together with the antenna. Although, demonstrating the full BJT model as it behaves in real life applications is not possible, one can approximate the circuit model according to the operating range. Since the matching circuit is not a high power system we can use the small signal model of BJT. Its equivalent circuit is given in Figure 3.3.

Now consider the NIC circuit with the antenna design. The time harmonic analysis of the matching and the antenna will be done on the equivalent circuit given in Figure 3.4. Using the Kirchhoff voltage law, we get from purely negative impedance

$$V_s = i(R_A + 1/j\omega C_A) - iZ_L \qquad (3.1)$$
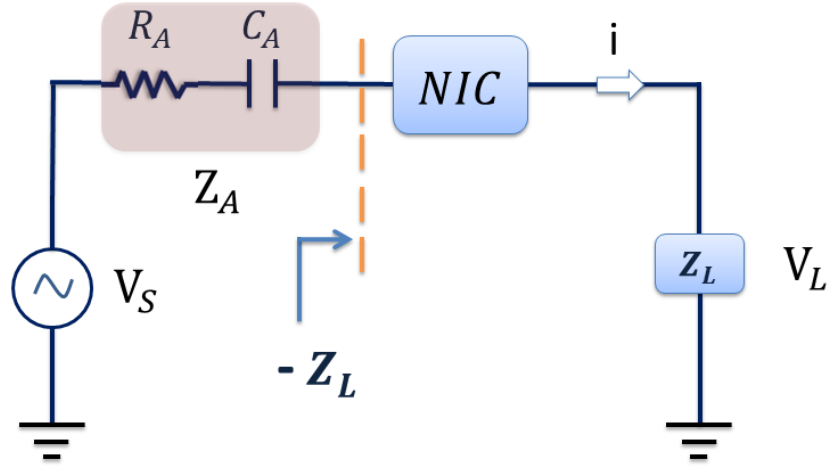
Solving for the current gives

26

Figure 3.4: Antenna Equivalent Circuit serially loaded by NIC circuit

$$i = \frac{V_S}{R_A + 1/j\omega C_A - Z_L} \tag{3.2}$$

Applying Ohm's Law, we get;

$$V_L = iR_L = \frac{V_S R_L}{R_A + 1/j\omega C_A - Z_L} \tag{3.3}$$

One can deduce that the maximum voltage and from that, maximum power could be achievable by opting for the negative impedance as a capacitor and equal to $(Z_L = 1/j\omega C_A)$. The NIC circuit provides negative of the load impedance at the input, therefore, we should take the load equal to the capacitance impedance value of the ESA. By doing so, we removed the reactance part of the antenna which caused a massive reduction in the receiver voltage.

3.3 Linvill's OCS and SCS design

The negative impedance convertor was first introduced using a transistor circuit by Linvill in 1954. The NIC circuit basically inverts the voltage across the ports

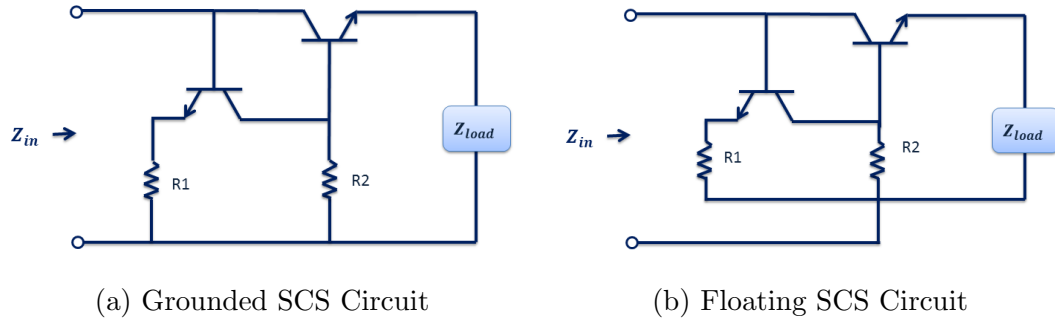(a) Grounded SCS Circuit   (b) Floating SCS Circuit

Figure 3.5: Linvill's SCS Circuit Designs

or the current flow into and out of the device, i.e. it creates an 180 degree phase shift between the input and the output of 2 port networks.

ESA has the disadvantage of low gain of a transmitting antenna and there is a need to increase the transmitter output power. Hence a larger input and prime power source are required to attain the desired output power for radiation. The NIC circuit is active, i.e. it inserts external power to the system. Such devices generally do not obey the Foster's reactance theorem and have a negative slope of impedance versus the frequency.

Linvill used bipolar junction transistors (BJT) in his works. He introduced negative resistance circuits using both grounded and floating NICs terminated as shown in Figure 3.6. He presented two types of circuit; open-circuit stable (OCS) and short-circuit stable (SCS). In order to make the concepts more understandable, consider a two port network like in the Figure 2.1. The impedance seen from one port can be defined as

$$Z(s) = \frac{V(s)}{I(s)} \tag{3.4}$$

If the network is driven by a voltage source, then the response to the excitation will be the current I(s)

$$I(s) = \frac{1}{Z(s)}V(s) \tag{3.5}$$

28

If one port of the system is stable and if zeros of the Z(s) are all in the left hand (LH) of the s-plane excluding the $j\omega$ axis, then the one port is called a **short circuit stable**(SCS) [33].

The one port is being driven by a current source, then the V(s) across its terminals given by;

$$V(s) = Z(s)I(s) \tag{3.6}$$

The system is **open circuit stable** (OCS) if Z(s) has a pole in the LH plane of the s-plane.

The NIC circuit can be simplified by representing the BJT's by a current source alone (neglecting capacitors). Small signal equivalent hybrid-π model given in the Figure 3.6c. By neglecting capacitor values, taking r_0 infinite and making appropriate calculations with ideal transistors($\beta \rightarrow \infty$), a pure negative input impedance is obtained as;

$$Zin = \frac{-R_1}{R2}Z_{load} \tag{3.7}$$

In Linvills actual realizations, a substantial reactive component of Z_{in} accompanies the negative resistance, resulting in a low Q-factor. An open circuit stable (OCS) circuit means, practically, that if a very large resistance terminates the negative-resistance one-ports on the left, then the overall network will be stable.

3.4   Circuit Design and Simulations

In this study, Linvill's OCS design is used as a basis. Idealized negative-image modeling ignores the practical implementation problems for negative elements. However, the NIC circuit design should be checked for transistor selection, biasing, noise, and the most crucial and difficult one is circuit stability.

Biasing is applying predetermined voltages or currents at various points of an electronic circuit with the aim of setting up proper operating conditions in circuit

(a) Grounded OCS Circuit
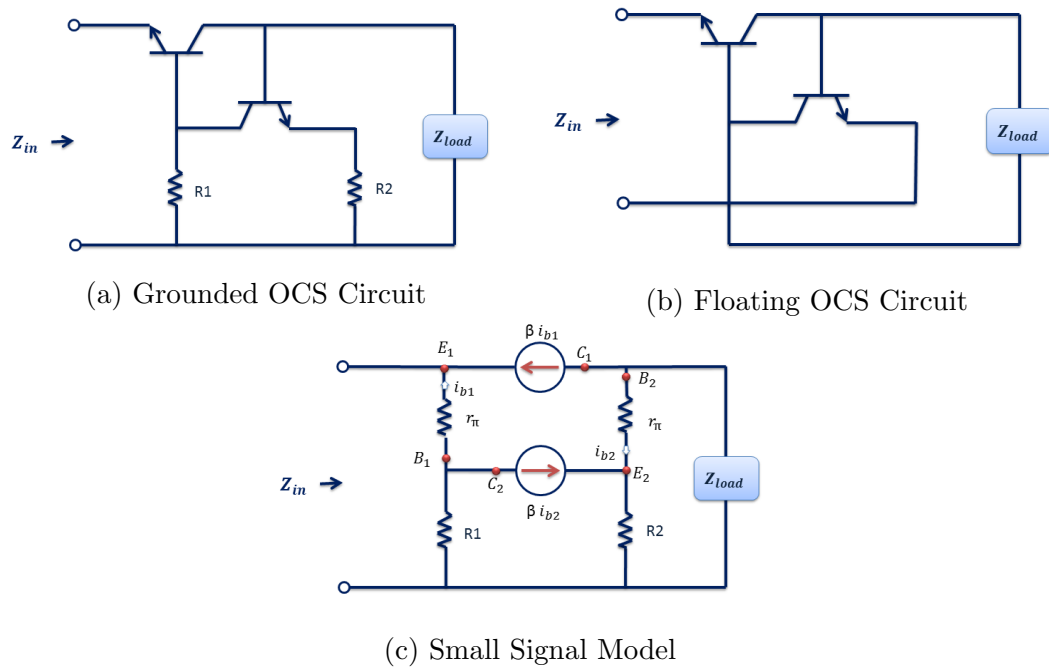
(b) Floating OCS Circuit

(c) Small Signal Model

Figure 3.6: Linvill's OCS Circuit Designs and Small Signal Equivalent Model

components. Transistor circuits use time-varying (AC) signals and also require a steady, time invariant, (DC) current or voltage to operate correctly. The AC signal applied to the circuit is superimposed on the DC bias current or voltage [34]. The operating point of a device, also known as the bias point, or quiescent (Q) point is the steady-state voltage or the current at a specified terminal of an active device with no input signal applied.

Figure 3.7 shows the designed circuit which matches the antenna to a 50 Ω transmission line. It behaves as a negative capacitor to cancel out the reactance part of an antenna. The circuit is connected to the ESA in parallel. In this figure the antenna is modelled as a 100pF capacitor and the 4 Ω resistor in a box which is terminated to input part of the NIC circuit. The total impedance of the ESA is named as Z_A. However, referring to Chapter 2, the input resistance of a dipole has frequency square dependency therefore a some error is expected. We held up an example of Sussman's paper [8] when constructing the circuit, however, our design also included resistive matching. On the left part of the design, the RC and RL circuit were designed to match a 50 Ω transmission line and they also serve as a tank circuit to control the operating frequency range. They transmit

the wanted signals and stop the unwanted. Coupling capacitors used to transmit only AC signals and block DC signals. They isolate the DC biasing and also protect the AC source from being damaged by the DC voltage leakage. As a transistor, the NEC NE85630 NPN BJT transistor model is chosen and its spice model is used in a simulation tool. Table 3.1 shows the missions of the each component briefly.

The constructed circuit was simulated in the Advanced Design System tool. It is an electronic design automation software for RF and microwave applications. In order to design the NIC circuit, DC, AC, transient, parametric and S-parameters solution features are used. The transistor spice model is directly imported from the website of the NEC to ADS.

Table 3.1: Mission of the Circuit Elements in Disk Loaded Dipole Antenna Model That Loaded by NIC Circuit

NIC	NPN1,NPN2
Antenna	C12, R11
Load	C9
Biasing	R3, R5, R6, L2, C4, C6
Filter	R1, R8, R9, R10, L1, L3, C7, C11
Coupling	C1
Feedback Control	R4,R7
Parasitic Element	C10
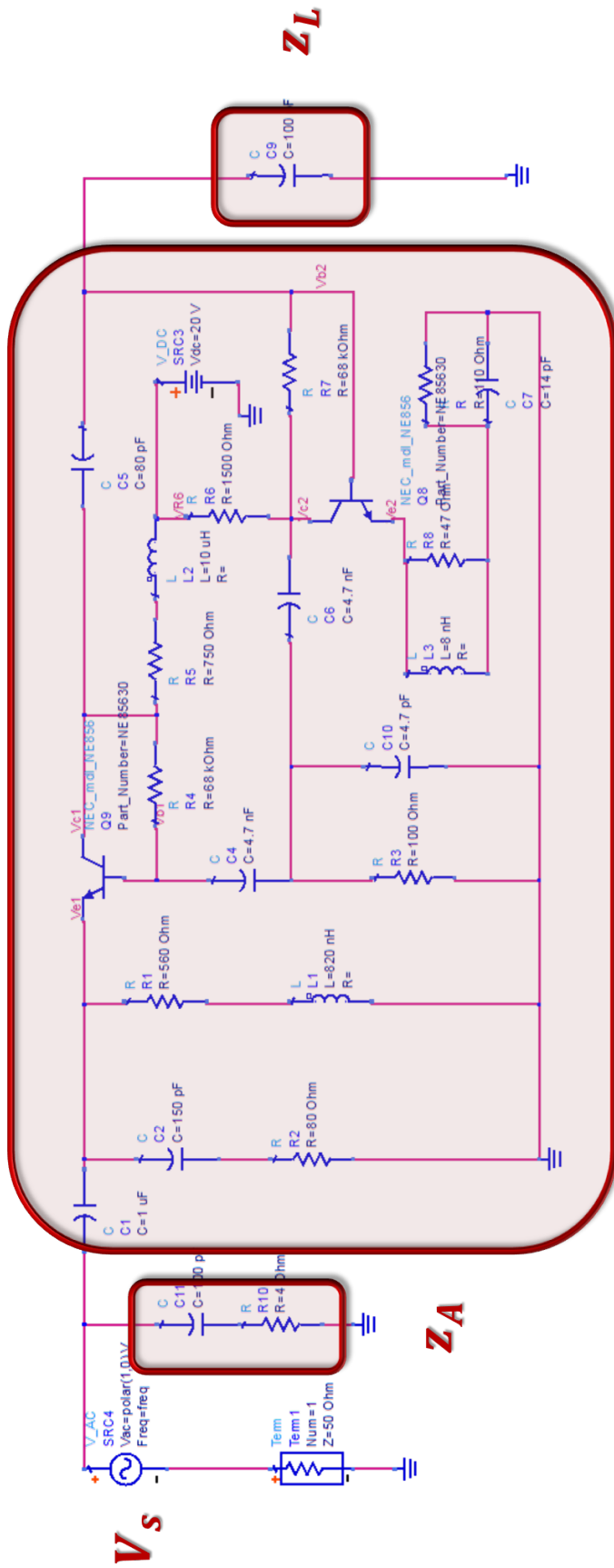
Figure 3.7: Disk Loaded Dipole Antenna Model Loaded by NIC Circuit

Chapter 4

Fabrication and Results

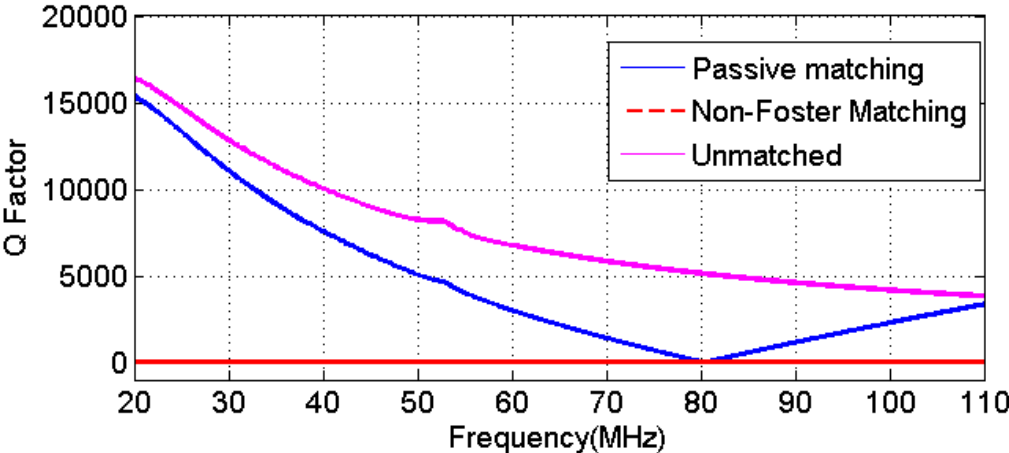## 4.1 Simulation Results of Active and Passive Matchings

Figure 4.1: Q Factors Comparison of Passive, Active and Unmatched Antenna

The Q-factor of the classical matching, non-Foster matching and unmatched case are simulated and the results are shown in Figure 4.1. The unmatched case, the disk loaded dipole antenna has a very high Q-factor which implies narrow bandwidth. As it is stated in Chapter 2, in order to increase bandwidth we need to decrease the Q-factor and for doing that we need an external matching circuit.

The first way to match the ESA is using the circuit which is constructed with passive elements. Since the ESA is highly capacitive, the inductor is connected to the one port of the ESA in order to cancel the negative reactive part of the terminal impedance. However, the passive matching compensates the reactance part only at a single frequency. Toward high-end and low-end of the frequency of interest, the Q-factor is increasing and also, it has tended to become larger than the unmatched case for higher frequency values. Consequently, using passive elements to match the ESA has the disadvantage of low operational bandwidth. The classic matching approximately has a 3 dB bandwidth of 1 MHz with a tolerable limit of 3:1 VSWR is satisfied (i.e. $\Gamma = 0.5$).

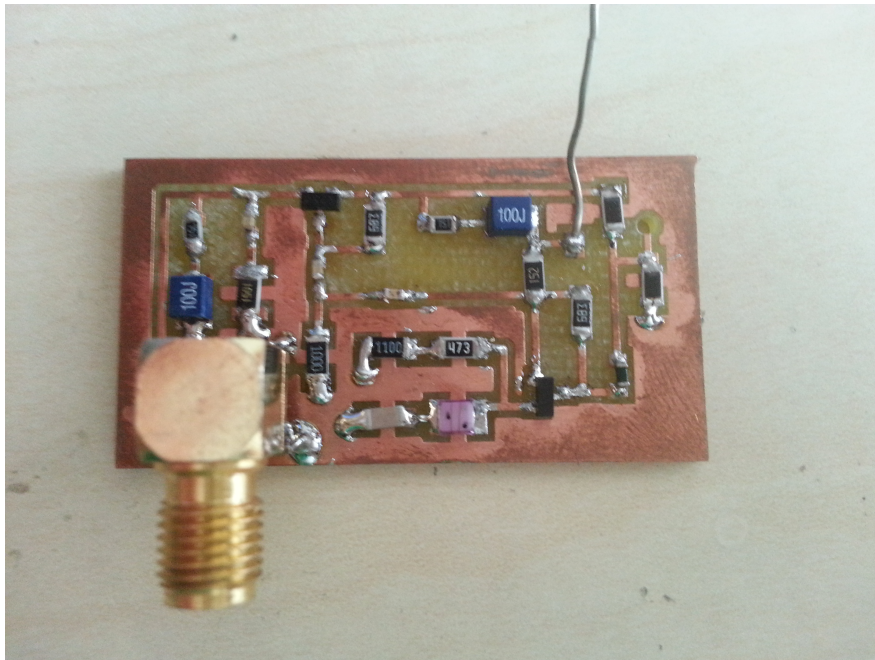## 4.2 Fabrication of the NIC Circuit

Figure 4.2: Fabricated Circuit on PCB Substrate

The circuit is printed on an RT/droid 5880 substrate and copper is used as a conductor. Surface-mount devices (SMD) opted for over through-hole components due to dimension concerns. They also have the advantages of lower resistances and inductances at the connections; consequently, fewer unwanted

34

RF signals affect the operation and a better, more predictable high-frequency performance is obtained. Moreover, the constructed circuit is more resistant to shocks and vibrations and therefore has a better mechanical performance. The measurements are taken from a Vector Network Analyzer and the S parameter analysis are carried out to calculate the input impedances, the Q-factor and the VSWR. Figure 4.2 shows the constructed circuit on a PCB. The dimensions are approximately 5 cm $\times$ 3 cm.

## 4.3   Results of the Non-Foster Matching

The simulation results of the NIC circuit loaded by disk loaded dipole are given in Figure 4.3. The equivalent circuit model of the ESA implemented as series capacitor and resistor which are connected in parallel with the NIC circuit. The NIC circuit provides a non-Foster match to the ESA, which matches the antenna very broad range of frequencies. Nearly, 3:1 VSWR is satisfied between 45 to 95 MHz in simulation. However, in measurements 3 dB bandwidth decreased to the value of 10 MHz with the same value of the VSWR. The obtained bandwidth is still a reasonable value for broadband applications.

The capacitive part of the antenna impedance is given in the Figure 4.3b. We obtain a negative capacitor to match the ESA, however, the reactance part of the input impedance could not be fully suppressed. Although, around the operation frequency the capacitance curves consistent with each other, for the frequencies lower than 30 MHz, At low frequencies the transistors cannot operate properly as also evident from the data sheet [35]. For high-frequency values, the circuit suffers from stability issues. In order to alleviate this issue and to provide sufficient amount of negative capacitance, high-frequency stabilization methods can be employed in order to enhance the performance at high-end of the frequency of interest, specifically around 100 MHz [8].
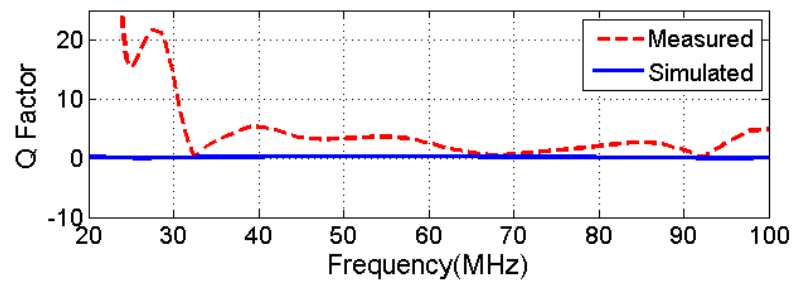
As it is inferred from the Figure 4.3b, the resistive value of the input impedance of the NIC circuit terminated with the disk loaded dipole antenna
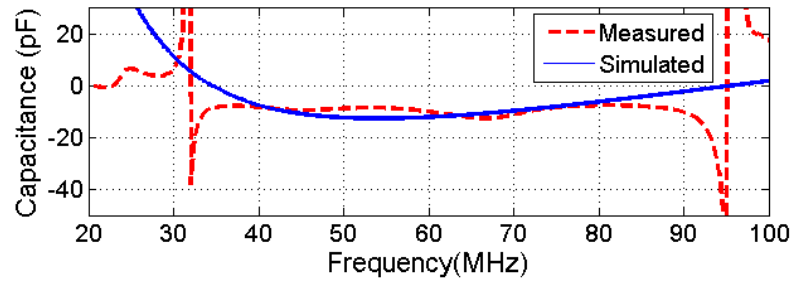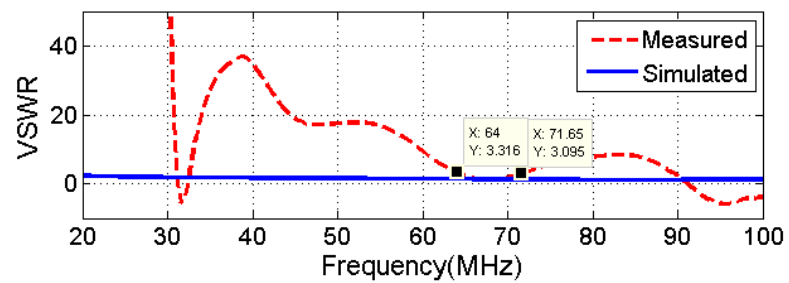
(a) Capacitance
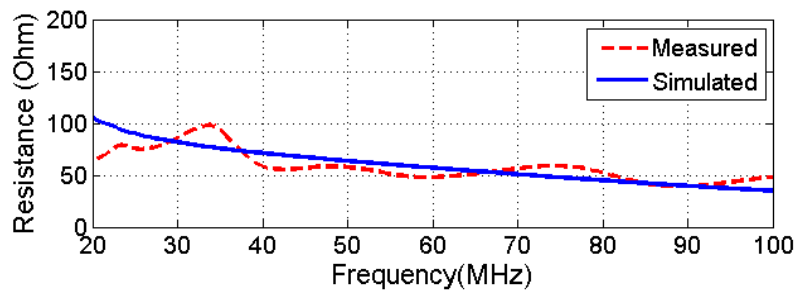
(b) Resistance

(c) Quality Factor

(d) VSWR

Figure 4.3: NIC circuit and loaded antenna simulation results

is matched to 50 ohm transmission lines at operating frequency 70 MHz. The resistive part of the terminal impedance shows a fair agreement with the measurement results, particularly for the frequencies between 50 MHz and 100 MHz. The agreement deviates as the frequency gets lower. Particularly for the frequencies lower than 30 MHz, the deviation is emphasized, which is again due to the transistor properties. As mentioned above, the transistor is not suited for the applications lower than 30 MHz.

Regarding the Q-factor and VSWR results extracted from measurement results, the high-end (100 MHz) and low-end (30 MHz) of the frequency bands show deviations compared to simulation results. Q-factor and VSWR results can be improved by using high-frequency stabilization methods and selecting a different transistor structure. The results of the Q-factor and the VSWR are illustrated in Figure 4.3c and 4.3d, respectively.

Another cause of error could be fabrication faults. The SMDs might be damaged during the soldering process. Also, the copper transmission lines are of a narrow design and this exerts the inductance into the system. Therefore, we obtain more negative capacitance values in measurements than simulations. Moreover, at ports, SMA connections are used and its leg lengths are wider than the copper lines and this can lead to mismatches which would increase the VSWR. Furthermore, in simulations, the connection and cable losses are not included which contribute the total error.

The error can be minimized by using more professional fabrication devices. In order to connect the SMDs, dye bonder or wire bonder can be used to avoid damaging the circuit elements during the soldering process. Also, the circuit elements could be chosen from the same class in order to have same pad dimensions which provides easiness for layout design and assembling process. Besides, instead of RT/droid 5880 more efficient substrate could be used.

4.4 Stability

After the proper design of the NIC circuit, a challenging task, though, it is important to analyze its stability. For this purpose, we will consider the complete system response and design circuits in such a way that a stable response is obtained for all time instants starting from the initial time. In the literature, various test methods have been suggested [36],[37],[38] and particularly, it has been established that two of the notable tests, i.e. Loop Gain and Llewellyn (or) Rollett, for analyzing the stability of Non-Foster circuits are unreliable and inaccurate because of their vulnerability leading to incorrect results [13].

In this work, we first use the open loop gain method to analyze the stability. Secondly, the results of the transient response analysis have been presented. In order to apply open loop gain method, an open loop system is required with the active device connected to load circuit. Since Linvill's OCS is used to design NIC circuit this condition is already satisfied. Then open loop gain can be found from

$$G = \frac{S_{21} - S_{12}}{1 - S_{11}S_{22} + S_{12}S_{21} - 2S_{12}} \qquad (4.1)$$

Figure 4.4 shows the open loop gain of the NIC circuit. According to Nyquist stability criteria, the gain is circulating in CW direction with the increase in frequency implying stability [39].

Transient analysis is applied as a secondary test in order to reinforce our results and compensate the inaccuracies that can arise in the open loop gain method. The transient response is applied for a very short period of time immediately after the system is turned on. If the system is unstable, the transient response will shoot rapidly with time, and in most cases the system will be practically unusable or even destroyed during the unstable transient response. The transient response should be carefully monitored since some undesired phenomena like high-frequency oscillations, rapid changes, and high magnitudes of the output may occur.
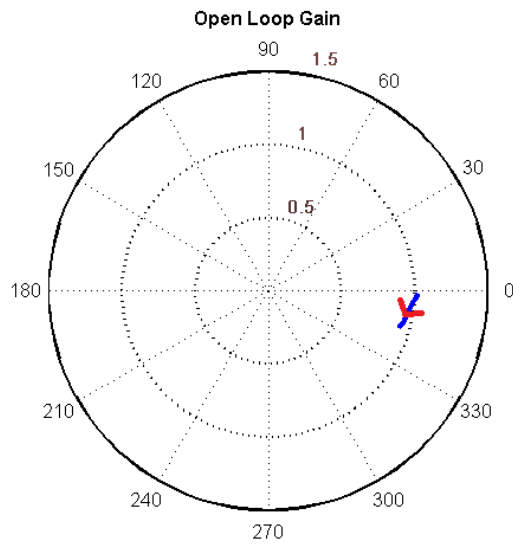
Figure 4.4: Open Loop Gain on Polar Plot

Figure 4.5 shows the transient response of the circuit for 100 millisecond. Although the transient voltage oscillates yet it is bounded by time. Therefore, the designed circuit is stable in the desired range of frequency. We can also observe that the AC signal applied from input, that oscillates between $\pm 1V$, is amplified at the output. Thus, the NIC circuit functions as an amplifier circuit as well.
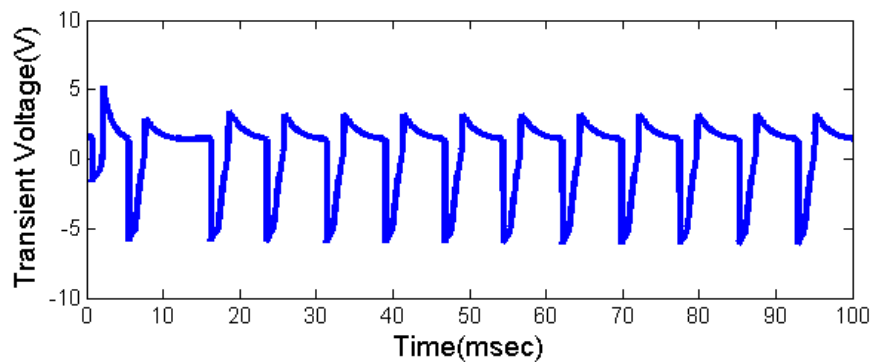

Figure 4.5: Transient Analysis of The Designed NIC Circuit for a Time of 100 msec

Chapter 5

Conclusion

The matching of electrically small antenna is becoming a major problem in miniature RF systems. The gain-bandwidth limitation puts constraints on the performance of the ESA. The NIC concept was introduced half a century ago and with the advances in transistor technology, it has attracted the attention of scientists and engineers. This matching circuit has the ability to cancel out the large reactance part of the ESA and hence, it overcomes gain-bandwidth limitation. In this thesis, the matching network for disk loaded dipole antenna is analyzed to demonstrate the feasibility of Non-Foster matching versus passive matching.

The objective of this thesis has been to understand the analysis of the practical issues of the application of non-Foster impedance matching with an NIC circuit. Component selection and proper biasing were very crucial in the establishment of the NIC circuit in order to operate the device in the appropriate range with intended specifications. The NIC circuit is designed according to the impact of supply voltage change and component model change, but the performance is not affected to a great extent due to this change. The variation of filter values has a significant effect on the design. Hence, choosing the bandpass and bandstop (notch) filter values is a necessary process. Moreover, these values also affect the stability of circuit design therefore multiple optimization steps are performed.

After appropriate design and simulation, the NIC matching circuit is fabricated and measured. By Non-Foster matching, an impressive enhancement in performance is achieved in the antenna operating range. The bandwidth of the matched antenna is 9 MHz wider, 10 times larger, than the passively matched antenna. The results are highly promising for broadband RF applications.

The NIC circuit cancels out the reactive part of the input impedance of the ESA, however, in complicated systems, it causes space, design and control complexity. Also, controlling the circuit requires a considerable amount of effort, hence, using a single negative element is rather preferable as opposed to using a non-Foster matching to cancel out the dominant capacitance of an ESA for narrow-band applications.

RF self-resonant antennas are very large and impractical. The work represented in this thesis, aims to contribute to the effectiveness and the broadband ESA design and matching. These antennas can be useful candidates for radios where the antenna size is a major problem. For a future study the antenna could be designed as a patch antenna and together with the NIC circuit, they can be fabricated on a single chip. Therefore, we can save a space and obtain a broadband, high gain antenna.

Bibliography

[1] R. C. Hansen, "Fundamental limitations in antennas," *Proceedings of the IEEE*, vol. 69, no. 2, pp. 170–182, 1981.

[2] A. Sridharan *et al.*, "Determination of q of small antennas," 2011.

[3] L. J. Chu, "Physical limitations of omni-directional antennas," *Journal of applied physics*, vol. 19, no. 12, pp. 1163–1175, 1948.

[4] H. A. Wheeler, "Fundamental limitations of small antennas," *Proceedings of the IRE*, vol. 35, no. 12, pp. 1479–1484, 1947.

[5] C. A. Balanis, *Antenna theory: Analysis And Design.* John Wiley and Sons, 2012.

[6] R. M. Foster, "A reactance theorem," *Bell System Technical Journal*, vol. 3, no. 2, pp. 259–267, 1924.

[7] S. E. Sussman-Fort and R. M. Rudish, "Non-foster impedance matching of electrically-small antennas," *Antennas and Propagation, IEEE Transactions on*, vol. 57, no. 8, pp. 2230–2241, 2009.

[8] S. E. Sussman-Fort, "Non-foster vs. active matching of an electrically-small receive antenna," in *Antennas and Propagation Society International Symposium (APSURSI), 2010 IEEE*, pp. 1–4, IEEE, 2010.

[9] H. Mirzaei and G. V. Eleftheriades, "Antenna applications of non-foster elements," in *Antenna Technology (iWAT), 2012 IEEE International Workshop on*, pp. 281–284, IEEE, 2012.

[10] S. Hrabar, I. Krois, I. Bonic, and A. Kiricenko, "Basic concepts of active dispersionless metamaterial based on non-foster elements," in *ICECom, 2010 Conference Proceedings*, pp. 1–4, IEEE, 2010.

[11] S. D. Stearns, "Non-foster circuits and stability theory," in *Antennas and Propagation (APSURSI), 2011 IEEE International Symposium on*, pp. 1942–1945, IEEE, 2011.

[12] E. Ugarte-Munoz, S. Hrabar, D. Segovia-Vargas, and A. Kiricenko, "Stability of non-foster reactive elements for use in active metamaterials and antennas," *Antennas and Propagation, IEEE Transactions on*, vol. 60, no. 7, pp. 3490–3494, 2012.

[13] S. D. Stearns, "Incorrect stability criteria for non-foster circuits," in *Antennas and Propagation Society International Symposium (APSURSI), 2012 IEEE*, pp. 1–2, IEEE, 2012.

[14] R. Elliott, E. Gillespie, *et al.*, "Ieee standard definitions of terms for antennas," *IEEE Transactions on Antennas and Propagation*, vol. 31, no. 6, p. 24, 1983.

[15] J. S. McLean, "A re-examination of the fundamental limits on the radiation q of electrically small antennas," *Antennas and Propagation, IEEE Transactions on*, vol. 44, no. 5, p. 672, 1996.

[16] R. F. Harrington, "Effect of antenna size on gain, bandwidth, and efficiency," *J. Res. Nat. Bur. Stand*, vol. 64, no. 1, pp. 1–12, 1960.

[17] I. T. Nassar, *Small Antennas Design for 2.4 GHz Applications*. PhD thesis, University of South Florida, 2010.

[18] V. Belevitch, "Summary of the history of circuit theory," *Proceedings of the IRE*, vol. 50, no. 5, pp. 848–855, 1962.

[19] B. Trevor, S, "Definition and misuse of return loss.," *Internet: http://ieeeaps. org/aps_trans/docs/ReturnLossAPMag_09. pdf [Accessed: 15 August 2010]*, 1990.

[20] F. Standard, "Glossary of telecommunication terms," *General Services Administration,Office of Information Resources Management*, 1986.

[21] E. Seeley, "An experimental study of the disk-loaded folded monopole," *Antennas and Propagation, IRE Transactions on*, vol. 4, no. 1, pp. 27–28, 1956.

[22] J. D. Kraus, "The helical antenna," *Proceedings of the IRE*, vol. 37, no. 3, pp. 263–272, 1949.

[23] R. Guertler, "Impedance transformation in folded dipoles," *Proceedings of the IRE*, vol. 38, no. 9, pp. 1042–1047, 1950.

[24] S. R. Best and D. L. Hanna, "A performance comparison of fundamental small-antenna designs," *Antennas and Propagation Magazine, IEEE*, vol. 52, no. 1, pp. 47–70, 2010.

[25] S. A. Schelkunoff and H. T. Friis, *Antennas: theory and practice*, vol. 639. Wiley New York, 1952.

[26] J. Maxwell, H. Poincaré, and F. K. Vreeland, *Maxwell's Theory and Wireless Telegraphy.* Archibald constrable and Company Limited, 1904.

[27] S. R. Best, "The radiation properties of electrically small folded spherical helix antennas," *Antennas and Propagation, IEEE Transactions on*, vol. 52, no. 4, pp. 953–960, 2004.

[28] M. Bern and D. Eppstein, "Mesh generation and optimal triangulation," *Computing in Euclidean geometry*, vol. 1, pp. 23–90, 1992.

[29] K. Fujimoto, *Small antennas.* Wiley Online Library, 1987.

[30] F.-f. Zhang, B.-h. Sun, K. He, P. Fei, and W.-j. Huang, "Study and design of a broadband monopole antenna using non-foster circuits," in *Antennas Propagation and EM Theory (ISAPE), 2010 9th International Symposium on*, pp. 60–63, IEEE, 2010.

[31] K.-S. Song and R. G. Rojas, "Electrically small wire monopole antenna with non-foster impedance element," in *Antennas and Propagation (EuCAP),*

2010 Proceedings of the Fourth European Conference on, pp. 1–4, IEEE, 2010.

[32] B. Van Zeghbroeck, "Principles of semiconductor devices," *Colarado University*, 2004.

[33] T. Deliyannis, Y. Sun, and J. K. Fidler, *Continuous-time active filter design.* Crc Press, 1998.

[34] P. R. Gray and R. G. Meyer, *Analysis and design of analog integrated circuits.* John Wiley & Sons, Inc., 1990.

[35] C. E. Laboratories, "Nec's npn silicon high frequency transistor," 2003.

[36] S. J. Mason, "Power gain in feedback amplifier," *Circuit Theory, Transactions of the IRE Professional Group on*, no. 2, pp. 20–25, 1954.

[37] M. Tian, V. Visvanathan, J. Hantgan, and K. Kundert, "Striving for small-signal stability," *Circuits and Devices Magazine, IEEE*, vol. 17, no. 1, pp. 31–41, 2001.

[38] J. Rollett, "Stability and power-gain invariants of linear twoports," *Circuit Theory, IRE Transactions on*, vol. 9, no. 1, pp. 29–32, 1962.

[39] R. Ludwig, *RF Circuit Design: Theory & Applications, 2/e.* Pearson Education India, 2000.

Appendix A

Implementation and Analysis of Sussman's work

This part of the study, Sussman's work presented in [8] is simulated and analyzed, also, its stability is checked with the transient solution method. In his work, Sussman tried to matched 2m long dipole with the non-Foster matching. His circuit behaves like -47pF capacitor. Figure A.2 gives the parameters of the designed circuit. In Figure A.2, the parameters of its design are obtained from the ADS simulation tool. After that, the stability of its circuit is checked from the open loop stable circuit and it is confirmed.
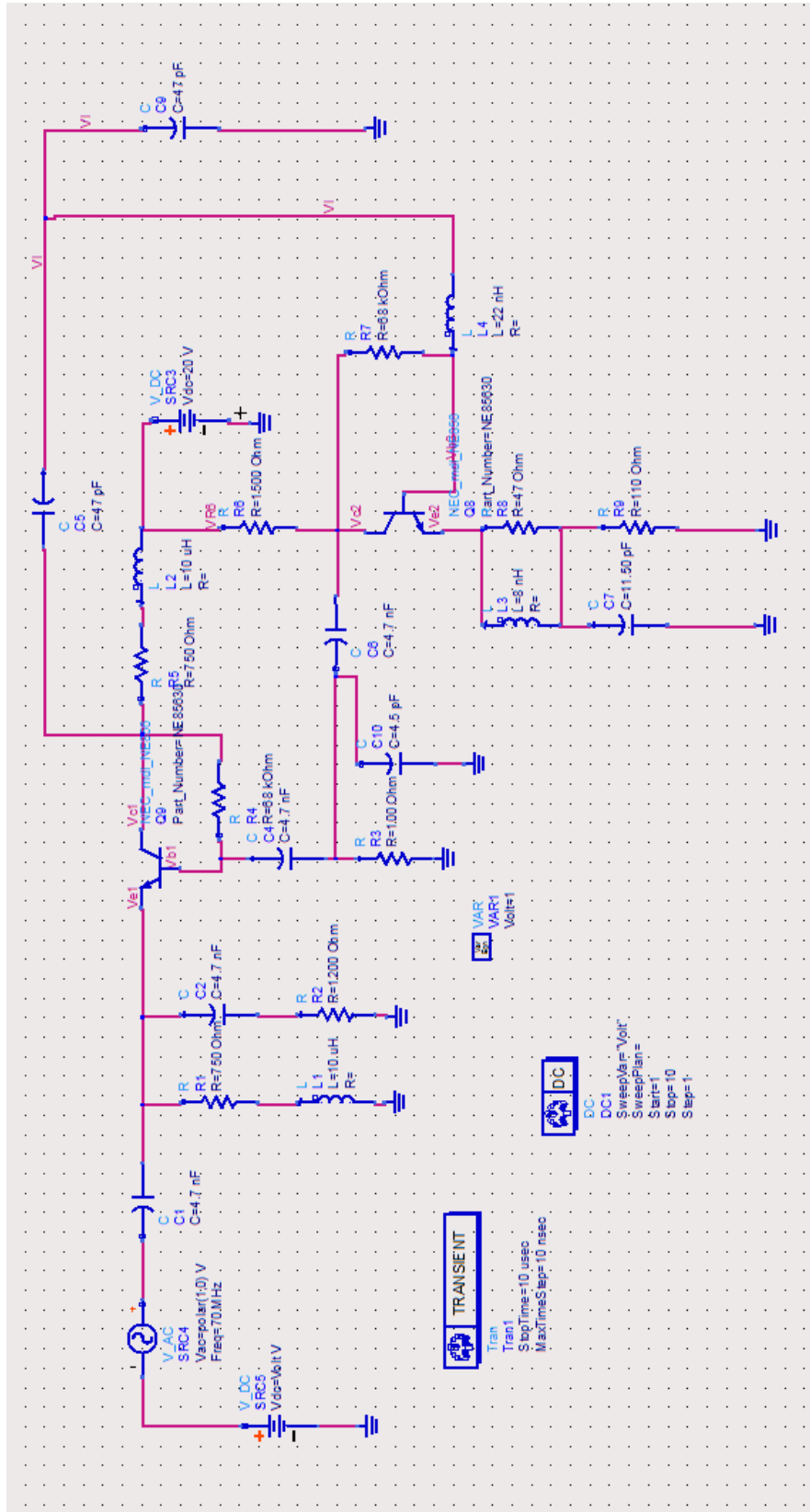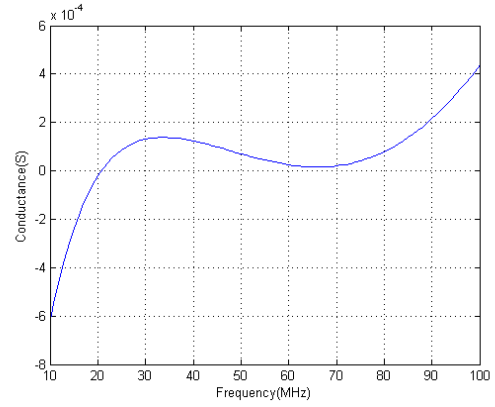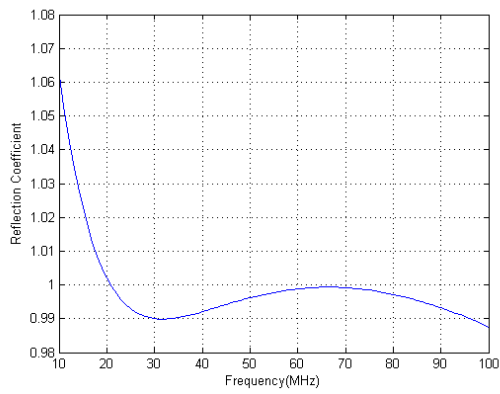
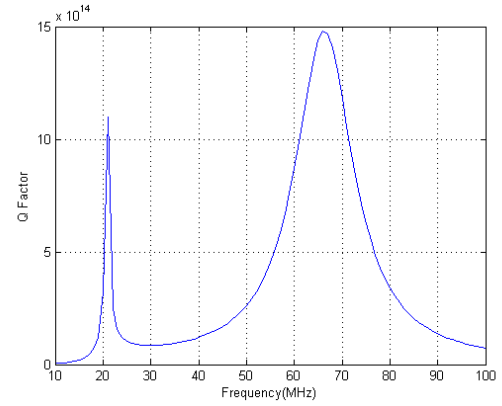Figure A.1: Sussman's NIC circuit design
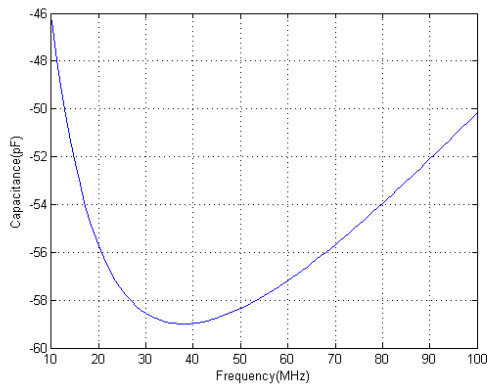
(a) Capacitance

(b) Conductance

(c) Reflection Coefficient

(d) Quality Factor
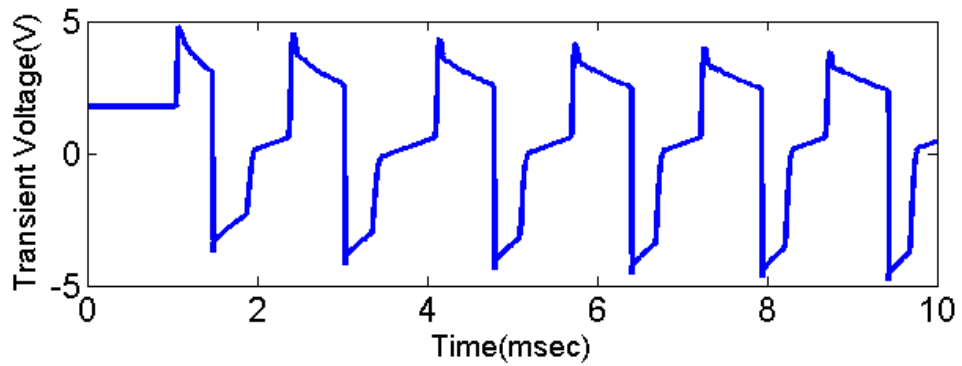
Figure A.2: Simulation of Sussman's work

Figure A.3: Transient Analysis of Sussman's NIC

Appendix B

Transistor Parameters

Spice Model

```
.MODEL NE85600 NPN
+(  IS=6e−16 BF=120 NF=0.978 VAF=10 IKF=0.08
+  ISE=32e−16 NE=1.93 BR=12 NR=0.991 VAR=3.9
+  IKR=0.17 ISC=0 NC=2 RE=0.38 RB=4.16
+  RBM=3.6 IRB=1.96e−4 RC=2 CJE=2.8e−12 VJE=1.3
+  MJE=0.5 CJC=1.1e−12 VJC=0.7 MJC=0.55 XCJC=0.3
+  CJS=0 VJS=0.75 MJS=0 FC=0.5 TF=10e−12
+  XTF=6 VTF=10 ITF=0.2 PTF=0 TR=1e−9
+  EG=1.11 XTB=0 XTI=3 KF=1.56e−18 AF=1.49 )
.ENDS
*
```